



The Ebert-Fastie Spectrometer Control Hardware and Software

F. Sigernes

University Courses on Svalbard (UNIS), Box 156, 9171 Longyearbyen, Norway.

1. Basic optics

This document describes the hardware and software that controls the Ebert – Fastie spectrometers at the Auroral Station in Adventdalen, Svalbard. The main components of the instrument are shown in Fig. 1.

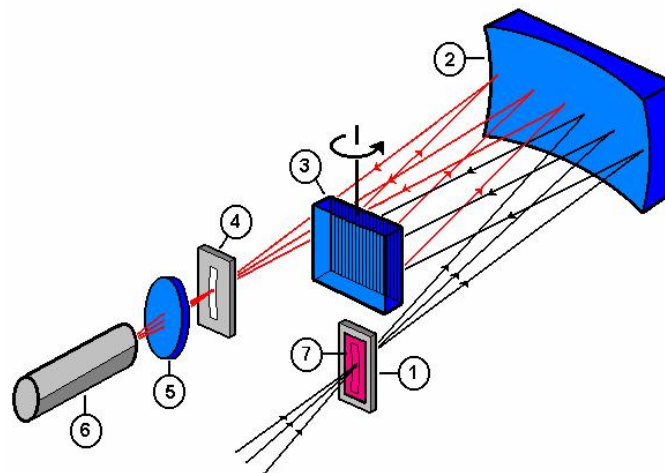


Figure 1. The Ebert-Fastie configuration: (1) entrance slit, (2) concave mirror, (3) plane reflecting grating, (4) exit slit, (5) collector lens, (6) detector, and (7) order sorting cut-off filter.

The principal components of the instruments are one large focal length spherical mirror, one plane reflective diffraction grating and a pair of curved slits. The recorded radiance from the sky is limited by the etendue - the product of the area of the entrance slit and the solid angle field of view. Because of the low intensity of the source, the etendue is made as large as possible. The image of the entrance slit is reflected by one part of the spherical mirror onto the grating. The second part of the mirror focuses the diffracted light from the grating onto the exit

UNIVERSITY CENTRE ON SVALBARD – P.O.BOX 156 – N-9171
LONGYEARBYEN NORWAY

slit. When the grating turns, the image of the entrance slit is scanned across the exit slit. A collector lens transfers the output of the exit slit to the front of a photomultiplier tube. The tube is mounted in a thermoelectrically cooled housing and cooled down to -20C. Signals from the tube are amplified and discriminated before sent to the computer's counting card. Cut-off filters are used in front of the entrance slit to prevent overlapping spectral orders. The field of view of approximately is approximately 5 degrees. Appendix A lists the fundamental equations for this type of optical configuration.

2. Short historical background

The original Ebert-Fastie spectrometer, was constructed by W. G. Fastie at John Hopkins University, Maryland at the beginning of the 70's. Fastie improved the original design of the monochromator made by Hermann Ebert in 1889. In 1978, a 1m and a ½m Ebert-Fastie spectrometer were transferred to the Auroral Station in Adventdalen, Svalbard, from the Geophysical Institute (GI), University of Alaska. One more 1m was installed in 1980. These instruments are named 1m Green, ½m Black and 1m Silver Bullet according to focal length and colour. Since then, the photon counting and computer electronics have been continuously upgraded in order to enhance both the control and performance of the instruments. Furthermore, a ½ m Ebert – Fastie spectrometer (½m White) was moved in 2004 from the Skibotn Observatory in Norway up to Longyearbyen. Data from these instruments are widely published and recognized.

The 1m Green and the ½m Black uses a high resolution stepper motor with encoder connected to the grating shaft. This is different from grating sweep mechanism (cam – arm system) used on the ½m White and 1m Silver Bullet. The steppers and encoders where installed in the early 90's. This document describes the 3rd software upgrade from DOS to Windows XP. The main reason for the latest software upgrade is that the old GI ISA counter cards from the 80's are out of production. The cards where made by Bruce McKibben and they where excellent! Nevertheless, ISA compatible computers are hard to get. A new PCI based card from the company National Instrument has now taken over.

3. Hardware overview

Fig. 2 shows the Ebert – Fastie spectrometer named 1m Green. The main electronics required to run the instrument may be separated in 4 sub categories

1. The detector head: photomultiplier tube (PMT), cooler and preamplifier / discriminator (PAD).
2. The high voltage supply.
3. The grating stepper - encoder motor system.
4. PC with high speed counter card.

A short description of each sub category follows.

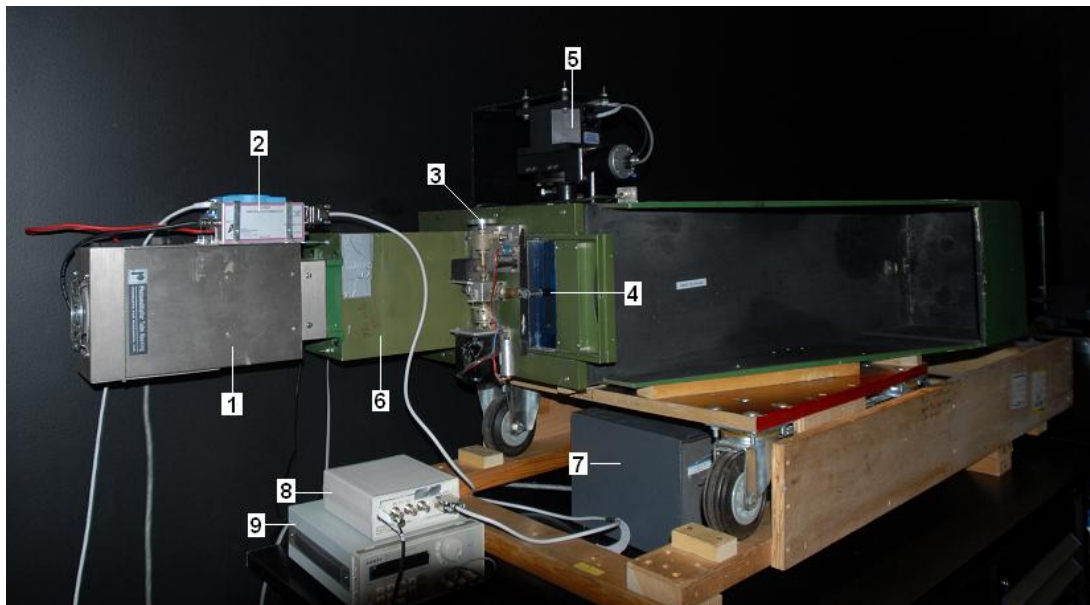


Figure 2. The 1m Green Ebert – Fastie spectrometer. (1) Peltier cooler for PMT, (2) PAD and High voltage controller (ADAM 6024), (3) Slit width adjuster wheel, (4) Order sorting filter in front of entrance slit, (5) Grating motor system, (6) Light pipe, (7) Power supply to cooler, (8) Power to PAD, and (9) DC supply to the ADAM module.

3.1 The detector head

In order to reduce thermo electrical noise or dark current, the photo-multiplier is cooled using the Peltier technique. Simply stated, Peltier cooling is based on the phenomenon of cooling or absorption of heat at the junction of two rods of metal or semi conductor when a current is made to pass through them. In order for thermoelectric cooling devices to be effective, the absorbed heat must be removed from the hot side of the device. In Fig. 2 an air fan is mounted on the top of the housing to blow out / exchange hot air.

The cooler in Fig. 2 is made by the company: Products for Research Inc, model number TE-102TS. Fig. 3 shows the PMT and the socket used. When a photon hits the photo emissive cathode of the tube, it emits a photoelectron into vacuum. The electron is then accelerated and directed to the first electrode (dynode), where it kicks loose a secondary electron. The process continues at the next dynode. Finally, the multiplied result, a train of electrons, is collected by the anode as an output signal. This is illustrated in Fig. 4. Most of the PMT's we use are from the Hamamatsu Corporation. Some old ones are from Thorn EMI, UK.



Figure 3. Detector: (1) Socket, (2) cooler and (3) photomultiplier (PMT).

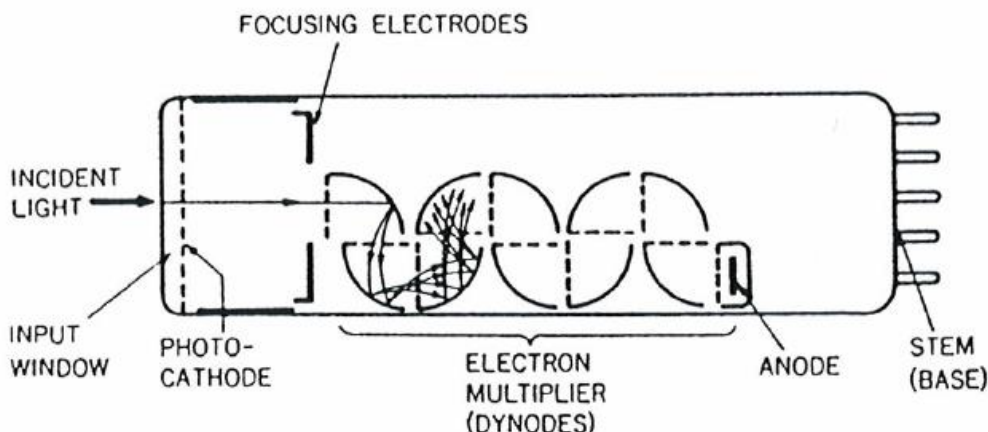


Figure 4. Basic principle of a photomultiplier (PMT).

The signals from the anode are amplified and discriminated to form a square pulse train. This operation is carried out by a PAD (Pulse Amplifier and Discriminator). The current pulses from the anode of the PMT are converted by the PAD to TTL compatible output pulses that are suitable for PC counter cards. Several types have been used from different manufactures. The Golden bricks are from the former company SpaCom Electronics, or the more recent Silver PADs are from Advanced Research Instrument Corporation, USA.

For the $\frac{1}{2}$ m White spectrometer, the PAD is actually mounted inside the socket, model ADS/ADH/ADP-120. This single printed circuit board comes with the socket from Products for Research Inc. Fig. 5 shows the F-100T Silver PAD and its main specifications.


	Max Repetition rate	50 MHz
	Sensitivity	160 μ V
	Input impedance	50 Ω
	Input noise level	5 μ V
	Pulse pair resolution	20 ns
	Min. output pulse width	10 ns
	Output	TTL
	Power supply (# F-100 PS)	+8 – 24 V

Figure 5. The F-100T Preamplifier / Discriminator from Advanced Research Instrument Corporation.

Due to availability and durability, we will use the Silver PAD for future upgrades.



Figure 6. High Voltage (HV)

3.2 The high voltage supply

The high voltage system to the PMT contains the actual high voltage generator, a signal control module and a couple of DC power supplies. The generator is produced by the company Euro Test in Germany (model # CPn 30 405 125). This unit is capable of producing up to -3kV. The output is controlled by a 12 channel multi purpose I/O module from Advantech Co., Ltd. The ADAM-6024 interfaces through the internet through standard IP- based protocols. Fig. 6 shows a close up of the ADAM module mounted on top of the high voltage generator. The PAD is mounted on the side of the modules. The specifications and the connection diagram are shown in appendix B and C, respectively.

3.3 The grating stepper - encoder motor system

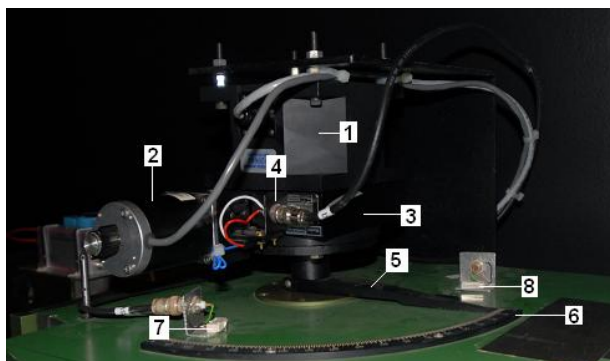


Figure 7. Grating stepper-encoder motor system: (1) encoder, (2) stepper motor, (3) gear drive, (4) home sensor, (5) grating normal (arm), (6) grating angle indicator, and (7 - 8) end - switches.

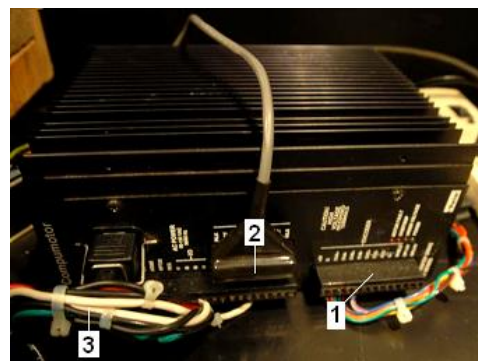


Figure 8. Motor drive indexer: (1) encoder connection, (2) stepper motor wire, and (3) to controlling PC (RS-232 COM 1).

Fig. 7 shows the motor system assembled to the 1m Green grating shaft. This motor is capable of doing 25,000 individual steps per revolution and is connected to a 5000 line encoder. The encoder shaft is mounted to a rotary table. The rotary table or gear drive has a gear ratio of 1:36 and is mounted directly to the grating shaft.

The whole system controlled by an Indexer that generates current pulses to drive the motor. See Fig. 8. The indexer provides additional logic such as limit switches and a home position switch. Homing is provided by a magnetic relay mounted on the rotary table. This custom made system is capable of doing 900,000 steps per revolution of the grating with exact position tracking.

It is possible to rotate the motor / grating to a precise position and stop, rotate at a constant velocity, alternate back and forth between two angular positions or use a combination of such moves.

The whole motor system was delivered by the Parker Hannifin Corporation, USA.

3.4 PC with high speed counter card



Figure 9. NI - PCI 6602

The counter card is made by National Instruments (NI). The NI 6602 device is a PCI bus compatible card. It has four 32-bit counter channels and up to 32 lines of individually configurable, TTL/CMOS-compatible digital I/O. The card has a base frequency of 80 MHz and each counter is capable of detecting down to 5 ns wide pulses. The card is installed on a Windows XP operated PC.

In addition, a NI SCB-68 connector box is used to access the cards ports. See appendix D for pin assignments.

Since the grating is fixed in position during sampling, a method called simple event counting is used. The counter (SOURCE) counts TTL pulses armed via a software command. The counter counts the number of falling edges that occur on SOURCE between two active edges triggered by software. At the completion of the period interval (Integration time P), the HW Save register latches the counter value for the software read. Fig. 10 shows an example of simple event counting where the counter counts 3 events on SOURCE.

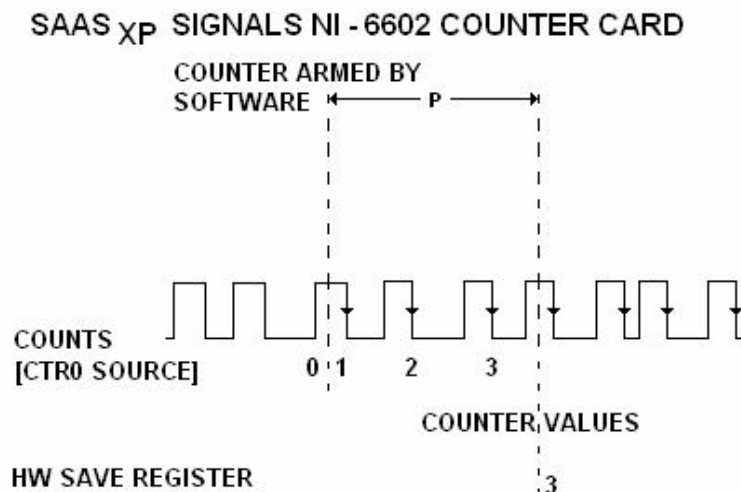


Figure 10. Simple event counting with the NI-PCI 6602 counting card

4. Software

4.1 SaasXP

The software to control the counter card is written in Borland Delphi 5. The routines used are developed over years of operating the spectrometers at the Auroral Station in Adventdalen, Svalbard. The platform is Windows XP. The program is called SaasXP, named according to its previous ancestors Saas and Spec4 that were compiled for DOS.

SaasXP uses the National Instruments driver library called NIDAQmx to communicate with the PCI NI-6602 counter card. These drivers are shipped with the card and need to be installed on the host computer. The library is accessible through the DDL file called *nicaiu.dll*. Here is an example on how to declare a function for use in Delphi:

```
function DAQmxStartTask(task: pointer):longint; stdcall; external 'nicaiu.dll';
```

In order to perform simple event counting as mentioned in the previous section, about 6 functions are called from the NIDAQmx library. See the source file *pmt_box.pas* for details. Appendix E lists an example on how the code can be written for sampling data.

The program is started by calling the main executable

```
D:\SaasXp\SaasXp 60
```

The input parameter 60 is optional and stands for runtime for a period of 60 minutes. This type of startup is ideal for scheduled operations, where different tasks may be required of the instrument.

Fig. 11 shows a screen capture of the program in operation. The program should be fairly easy to use. An explanation on how to use it is indicated by labels. The program remembers its position and size. Runtime status information is provided in the two status bars. A LED indicates whether the shutter is open or not. A toolbar at the top of the form contains buttons for documentation (shortcut to this file), a command prompt for high voltage control, copy to clipboard or printer, instrumental settings and enable or disable of recording (RUN button).

Note that the program remembers the status of the RUN button. If it is enabled during shutdown, then it will automatically start the instrument on the next execution. Shutdown is done 4 ways. Either by hitting the Esc button (fast or hard shutdown), by closing the main form (mouse click on upper right corner), disable the RUN button or by timeout as described earlier.

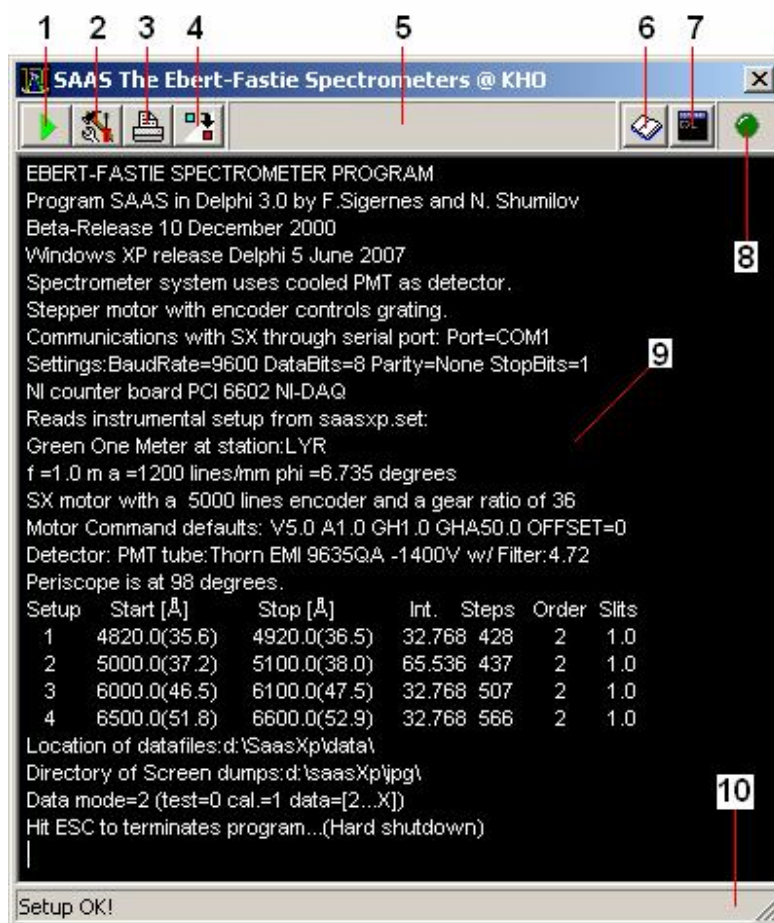


Figure 11. Screen capture of SpaasXp.exe. (1) is record or RUN button, (2) Setup / Configuration of instrument, (3) dumps current view to a printer, (4) copies to clipboard (print screen option), (5) status bar, (6) information (this file), (7) command prompt for high voltage, (8) shutter LED, (9) current settings of instrument, and (10) status bar.

The current setup of the instrument is listed as read only in the program when the instrument operates. In order to change the setup it is necessary to first disable the play button and then click on the setup button. This will open up a file called *SaasXp.set*. You will need to save this file to update the settings of the instrument. Fig. 12 shows the content of this file.

The configuration file is divided into 2 sections. First the instrumental or fixed settings are given by the specifications of the instrument. This section contains parameters such as site tag, name of instrument, photomultiplier tube, type of order sorting filter, grating groove density, focal length of mirror, motor-encoder settings, default plot options, and data location. Note that the format of the file must be conserved. All input must be placed correctly after the semicolon of each line. Any incorrect input will cause the program to crash. Keep one sample file as backup in case of problems.

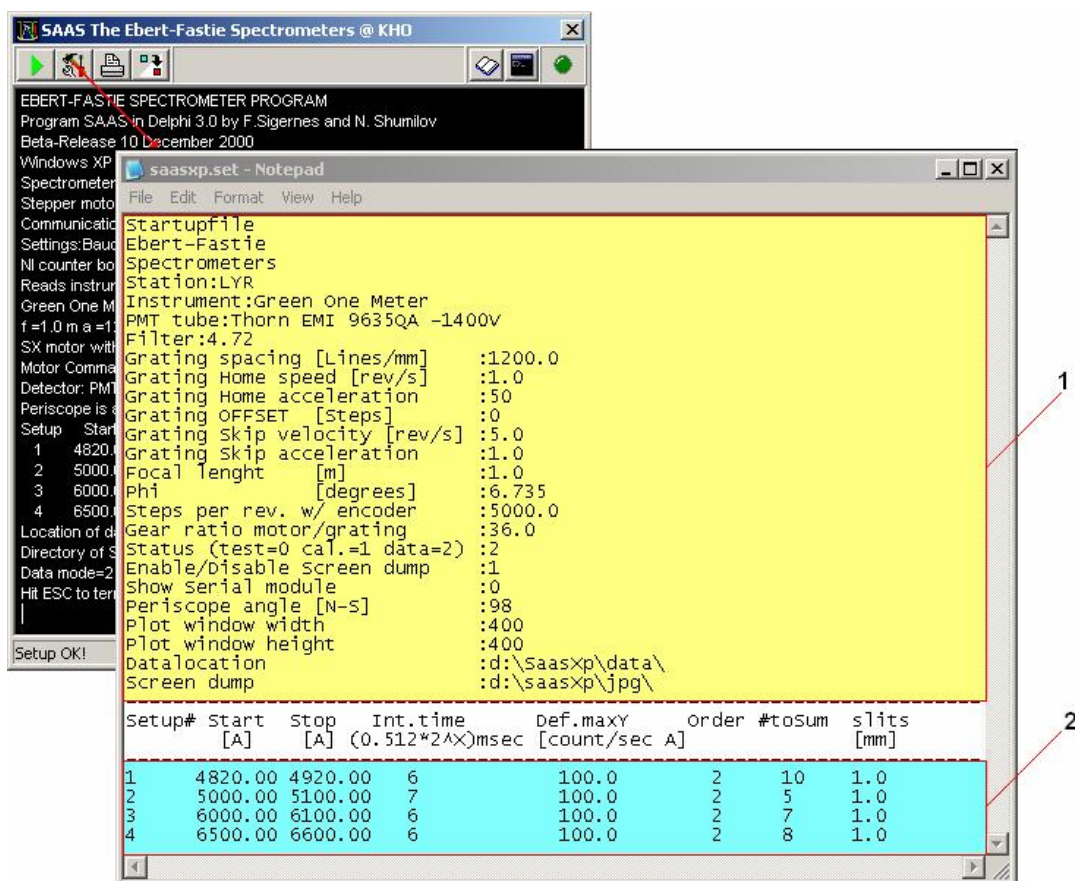


Figure 12. Configuration. The blocks (1) and (2) are colored yellow and light blue to visualize difference between fixed settings of the instrument and user runtime settings, respectively.

Secondly, the wavelength regions that the instrument will sweep are given in the runtime section of the configuration file. See block colored light blue in Fig. 12. Each region the instrument sweeps in wavelength is given as one line. The line starts with a setup number followed by a start and a stop wavelength, the integration code, a plot window maximum, the spectral order, the number to sum and the slit widths.

The integration code is entered according to the following table.

Code	0	1	2	3	4	5	6	7	8	9
msec	0.51	1.02	2.05	4.10	8.19	16.38	32.77	65.54	131.07	262.14

Again, it is important to enter the correct format. Also, each region should be entered according to a continuous increase in grating angle. This angle is given by the grating equation of the instrument and depends on spectral order (appendix A). In Fig. 11 the message “Setup OK!” in the status bar indicates that this rule has been followed. Numbers in parentheses next to the wavelengths give the calculated grating angles. If this rule is not obeyed, the program will just simply terminate.

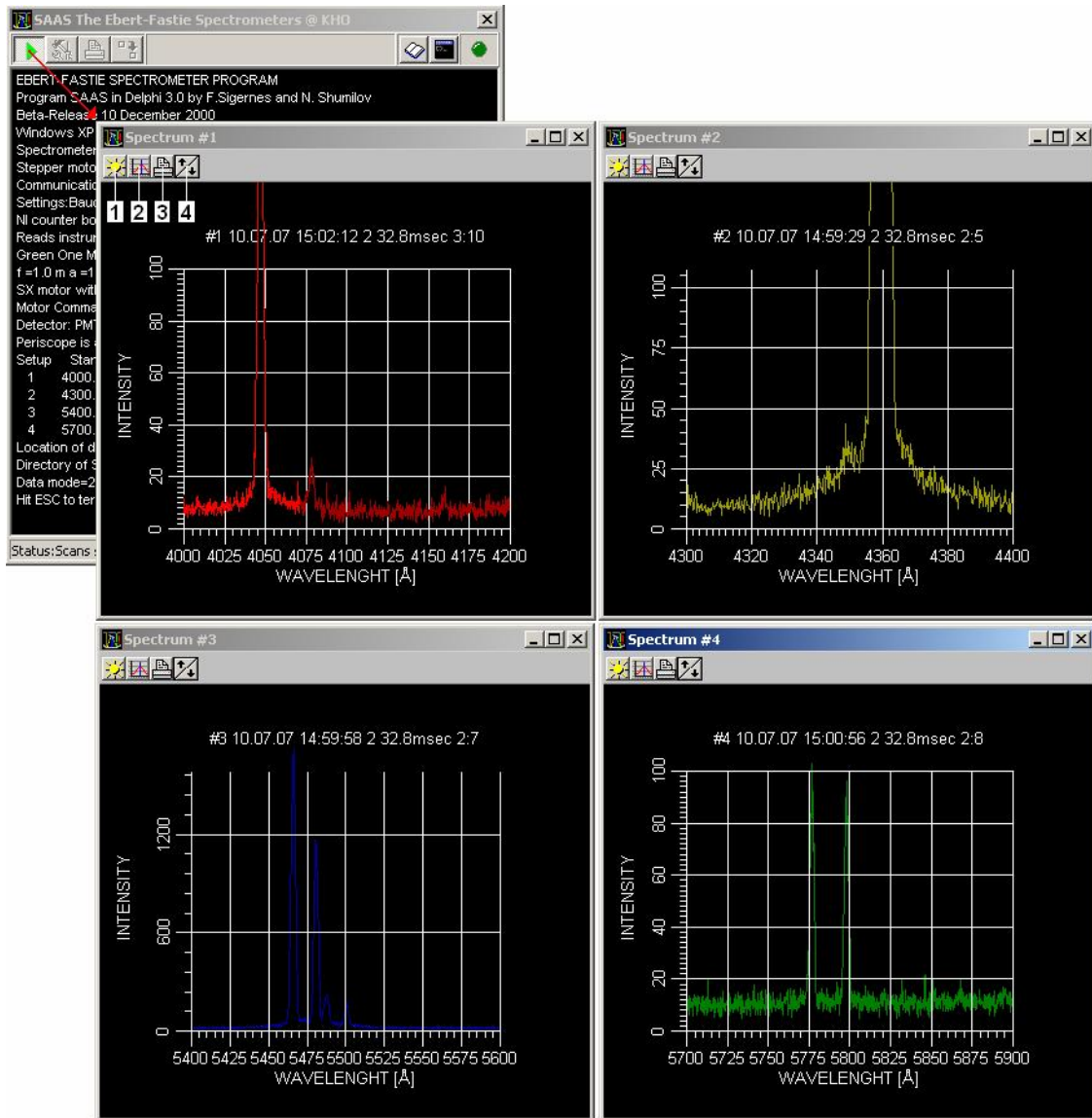


Figure 13. The figure shows the screen dump of SaasXp in action with 4 plot windows for each spectral region. Each plot is the runtime mean spectrum in units of raw counts and Ångström for intensity and wavelength, respectively. The labels are (1) – copy to clipboard, (2) – plot grid ON / OFF, (3) – print, and (4) – scale intensity axis up or down (maximum intensity value).

Note that it is only possible to define maximum 4 wavelength regions to sweep with SaasXp. Each region will produce its own plotting window. Fig. 13 shows the graphical layout of the plot windows. The main feature is that they plot wavelength versus intensity in real time. Bright colors indicates the current scans and corresponding darkened colors is the previously scans. The effect of the runtime mean is seen as an increase in signal to noise between scans. The # 2 sum does not influence the data saved to disk. Each individual scan is saved to file. The files are named according to date and saved in a directory selectable to the user. The format is simple ASCII.

UNIVERSITY CENTRE ON SVALBARD – P.O.BOX 156 – N-9171
LONGYEARBYEN NORWAY

Wavelength and absolute calibrations are conducted with the program *Spekkis.exe*, which is part of the distribution. The accurate start and stop wavelengths of the scan are calculated by the wavelength calibration module of *Spekkis*.

4.2 HvIP3

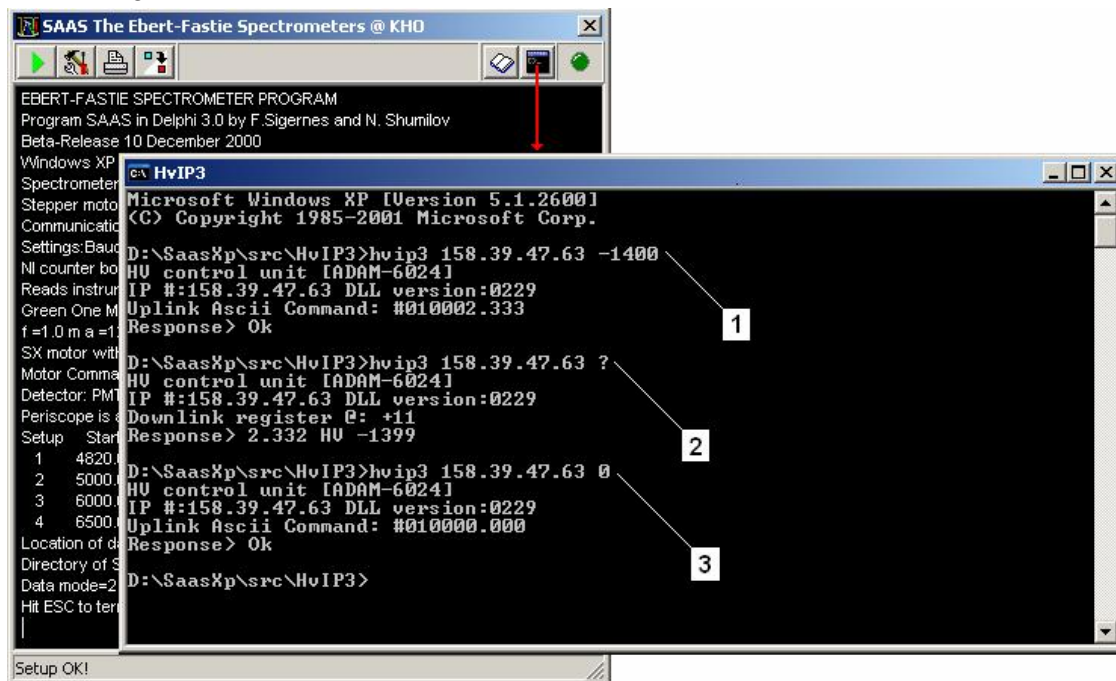


Figure 14. Screen shot of HvIP3 in action. Commands: (1) turns high voltage ON, (2) is status, and (3) turns the high voltage OFF. A four line response follows each command.

The *HvIp3.exe* is a command line program that communicates with the high voltage control module (ADAM-6024) via the internet. The program syntax is

Usage: `HvIp3 [IP:] [NEG PMT Voltage or ?]`.

To turn ON the high voltage to -1400V, simply type on the Command Prompt:

```
HvIp3 158.39.47.63 -1400
```

Correspondingly, the high voltage is turn OFF by the command

```
HvIp3 158.39.47.63 0
```

You request the status by typing

```
HvIp3 158.39.47.63 ?
```

Note that in the above examples the IP number 158.39.47.63 is just used for testing of the system. The program basically converts the input strings to the ASCII or the Modbus TCP/UDP protocols used by the manufacturer. The Delphi 5 source file *HvIP3.dpr* communicates with the Winsock API through the driver files *Adamtcp.pas* and *Adamtcp.dll* that comes with the unit. Two command files may be used to turn the high voltage ON and OFF in incremental voltage steps, respectively. Fig. 14 shows a screenshot of the program in action.

IMPORTANT

Turn the blue button of DC power supply to the high voltage unit OFF during troubleshooting or faulty conditions! Make sure that the ADAM module is operative and working before turning the power ON again (+12.5 VDC).

Manufactory list

Parker Hannifin Parker

Compumotor Division, 5500 Business Park Drive, Rohnert Park, CA 94928, USA
Phone +1 707-584-7558 or 800-358-9068
<http://www.parkermotion.com/>

Products for Research Inc.

88 Holten Street, Danvers, MA 01923, USA
Phone: (978)774-3250 – Fax: (978) 762-3593
<http://www.photocool.com/>

Hamamatsu Photonics K. K.

325-6, Sunayama - cho, Hamamatsu City, Shizuoka Pref., 430-8587, Japan
Phone: (81)-53-452-2141 – Fax: (81)-53-456-7889
<http://www.hamamatsu.com>

Advanced Research Instruments Corporation

PO Box 7427
Golden CO 80403 USA
<http://www.aricorp.com>

Euro Test

ET System electronic GmbH
Hauptstr. 119 – 121
D-68804, Altlußheim, Germany.
Tel.: +49 (0)6205 3948-0 - Fax: +49 (0)6205 375 60
<http://www.ETSGmbH.de>

Advantech Co., Ltd.

No. 1, Alley 20, Lane 26
Rueiguang Road, Neihu District
Taipei 114, Taiwan, R. O. C.
<http://www.advantech.com>

National Instruments

11500 North Mopac Expressway
Austin, Texas 78759-3504 USA
Tel: 512 794 0100
<http://www.ni.com/>

APPENDIX A

Basic equations for an Ebert-Fastie spectrometer

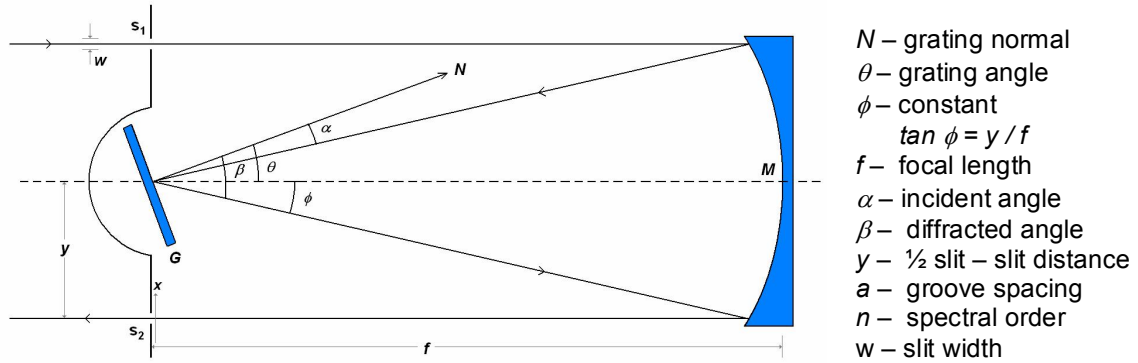


Figure 1. Optical diagram Ebert- Fastie spectrometer. G is plane reflective grating, S_1 entrance slit, S_2 exit slit, and M concave mirror.

The grating equation is

$$n\lambda = a (\sin \alpha + \sin \beta), \text{ where } \alpha = \theta - \phi \text{ and } \beta = \theta + \phi.$$

Then $n\lambda = a [(\sin \theta \cos \phi - \sin \phi \cos \theta) + (\sin \theta \cos \phi + \sin \phi \cos \theta)]$ or

$$\Rightarrow n\lambda = 2a \sin \theta \cos \phi.$$

Angular dispersion is

$$\frac{d}{d\beta}(n\lambda) = a \cos \beta,$$

and since $dx = f d\beta$ then linear dispersion becomes

$$\frac{d\lambda}{dx} = \frac{d\lambda}{d\beta f} = \frac{a \cos \beta}{nf} = \frac{a \cos(\theta + \phi)}{nf}$$

The theoretical bandpass of the instrument is then defined as

$$BP = FWHM = \frac{d\lambda}{dx} \times w = \frac{a \cos(\theta + \phi)}{nf} \times w.$$

APPENDIX B

CPx¹ 30 405 12 5

HV-Modul der CPS Serie

Technische Daten

V_{OUT}	$V_{X=p}$: 0 bis 3 kV $V_{X=n}$: 0 bis -3 kV	(bezogen auf GND)
I_{OUTmax}	4 mA	
V_{IN}	11,5 bis 15,5 V-DC	
I_{IN}	< 1,5 A ($V_{OUT}=0$; $I_{OUT}=0$: < 100 mA)	
Steuerung mit	$V_{SET} = 0$ bis 5 V	
Monitoring mit	$V_{MON} = 0$ bis 5 V	
Ripple	typ: 60 mV _{P-P}	max.: 150 mV _{P-P}
Stabilität	$\Delta V_{OUT} / \Delta V_{IN}$: < $1 \cdot 10^{-4} \cdot V_{OUTmax}$ Leerlauf/Vollast: < $2 \cdot 10^{-4} \cdot V_{OUTmax}$	
Temperaturkoeffizient	< $1 \cdot 10^{-4} / K$	
Betriebstemp.-bereich	0 ... +50 °C	
Lagertemp.-bereich	-20 ... +60 °C	
HV-Ausgang	- Lemo HV-Kabel 9 kV, geschirmt (LEMO 9106330) - Länge = 600 mm - Überlast und kurzschlußfest	
9-poliger D-Sub Stecker		
PIN	Name	Beschreibung
1	PWR_0V	Power 0 V (verbunden mit PIN 6, GND und Gehäuse)
2	V_{MON}	Monitorspannung entsprechend I_{OUT} $I_{OUT} = 0$ bis I_{OUTmax} \Rightarrow $V_{2-6} = 0$ bis V_{MON}
3	INH	INHIBIT (TTL-Pegel, LOW=aktiv \Rightarrow $V_{OUT} = 0$)
4	V_{ISET}	Hardwarestrom-Limit: $V_{4-6} = 0$ bis V_{SET} ($R_i = 10$ k Ω gegen V_{REF}) \Rightarrow $I_{OUT} = 0$ bis I_{OUTmax} n.c. \Rightarrow I_{OUTmax} ist möglich
5	PWR_+	+ V_{IN}
6	V_{SET_0V}	Signal 0 V (verbunden mit PIN 1, GND und Gehäuse)
7	V_{MON}	Monitorspannung entsprechend V_{OUT} $V_{OUT} = 0$ bis V_{OUTmax} \Rightarrow $V_{7-6} = 0$ bis V_{MON}
8	V_{VSET}	Spannungssteuerung: $V_{8-6} = 0$ bis V_{SET} \Rightarrow $V_{OUT} = 0$ bis V_{OUTmax}
9	V_{REF}	$V_{9-6} = 5$ V (1 mA) Interne Ref.-spannung für ext. Poti (Schleifer an V_{VSET} und/oder V_{ISET})

ET System electronic GmbH
Hauptstr. 119-121
D - 68804 Altlußheim Germany

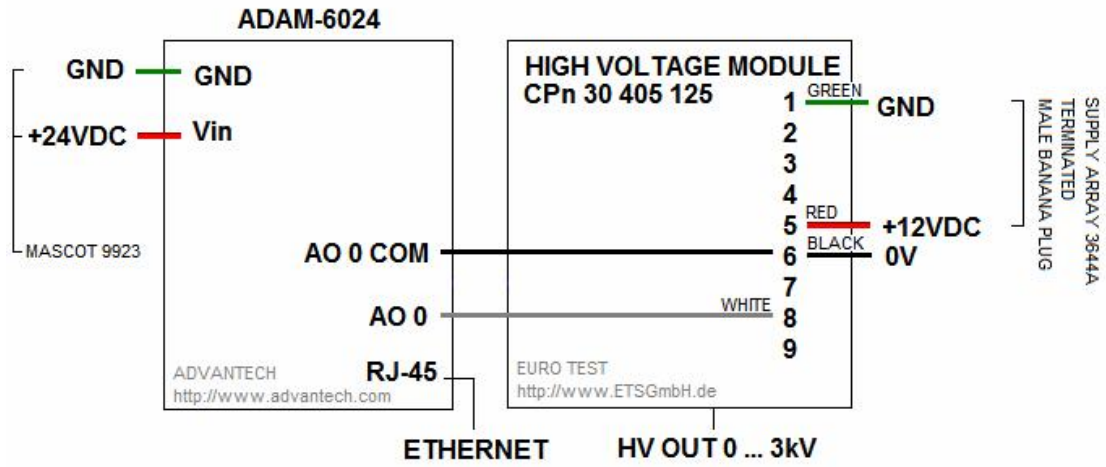
Email: info@ETSGmbH.de
http://www.ETSGmbH.de

Tel ++ 49 (0)6205 / 39 48 * 0
Fax ++ 49 (0)6205 / 37 560

UNIVERSITY CENTRE ON SVALBARD – P.O.BOX 156 – N-9171
LONGYEARBYEN NORWAY

APPENDIX C

HIGH VOLTAGE CONNECTIONS



APPENDIX D

SCB-68 Quick Reference Label

NATIONAL INSTRUMENTS 660X SERIES

If using a 6602 device with an optional SCB-68 shielded connector block accessory, affix this label to the inside of the SCB-68 and set the switches as shown below.

P/N 185974A-01

SET SWITCHES AS FOLLOWS FOR 6602 DEVICES.

<table style="display: inline-table; border-collapse: collapse;"> <tr><td style="width: 10px; height: 10px; border: 1px solid black;"></td><td style="width: 10px; height: 10px; border: 1px solid black;"></td><td style="width: 10px; height: 10px; border: 1px solid black;"></td></tr> <tr><td style="width: 10px; height: 10px; border: 1px solid black;"></td><td style="width: 10px; height: 10px; border: 1px solid black;"></td><td style="width: 10px; height: 10px; border: 1px solid black;"></td></tr> </table>							S1	<table style="display: inline-table; border-collapse: collapse;"> <tr><td style="width: 10px; height: 10px; border: 1px solid black;"></td><td style="width: 10px; height: 10px; border: 1px solid black;"></td><td style="width: 10px; height: 10px; border: 1px solid black;"></td></tr> <tr><td style="width: 10px; height: 10px; border: 1px solid black;"></td><td style="width: 10px; height: 10px; border: 1px solid black;"></td><td style="width: 10px; height: 10px; border: 1px solid black;"></td></tr> </table>							S2
<table style="display: inline-table; border-collapse: collapse;"> <tr><td style="width: 10px; height: 10px; border: 1px solid black;"></td><td style="width: 10px; height: 10px; border: 1px solid black;"></td><td style="width: 10px; height: 10px; border: 1px solid black;"></td></tr> <tr><td style="width: 10px; height: 10px; border: 1px solid black;"></td><td style="width: 10px; height: 10px; border: 1px solid black;"></td><td style="width: 10px; height: 10px; border: 1px solid black;"></td></tr> </table>							S5 S4 S3								

Application Contexts:

Counter
As shown on label

DIO (n= 0..31)
DIO_0 maps to PFI_0
DIO_n maps to PFI_n

Motion Encoder (n= 0..7)
SOURCE_n maps to CH_A_n
UP_DOWN_n maps to CH_B_n
GATE_n maps to CH_Z_n

See 6602 User Manual for details.

PIN#		SIGNAL		PIN#		SIGNAL	
68	GND						
34	PFI_31 (SOURCE_2)	12	PFI_3	1	+5V		
67	PFI_30 (GATE_2)	46	GND	35	RG		
33	GND	13	PFI_4	2	PFI_39 (SOURCE_0)		
66	PFI_29 (UP_DOWN_2)	47	PFI_5	36	GND		
32	PFI_28 (OUT_2)	14	GND	3	PFI_38 (GATE_0)		
65	GND	48	PFI_6	37	RESERVED		
31	PFI_27 (SOURCE_3)	15	PFI_7	4	RESERVED		
64	PFI_26 (GATE_3)	49	GND	38	RESERVED		
30	GND	16	PFI_8 (OUT_7)	5	PFI_36 (OUT_0)		
63	PFI_25 (UP_DOWN_3)	50	GND	39	GND		
29	PFI_24 (OUT_3)	17	PFI_9 (UP_DOWN_7)	6	PFI_33 (UP_DOWN_1)		
62	GND	51	PFI_10 (GATE_7)	40	PFI_37 (UP_DOWN_0)		
28	PFI_23 (SOURCE_4)	18	GND	7	PFI_35 (SOURCE_1)		
61	PFI_22 (GATE_4)	52	PFI_11 (SOURCE_7)	41	GND		
27	GND	19	RG	8	PFI_34 (GATE_1)		
60	PFI_21 (UP_DOWN_4)	53	PFI_12 (OUT_6)	42	GND		
26	PFI_20 (OUT_4)	20	GND	9	PFI_32 (OUT_1)		
59	GND	54	PFI_13 (UP_DOWN_6)	43	RG		
25	PFI_19 (SOURCE_5)	21	PFI_14 (GATE_6)	10	PFI_0		
58	PFI_18 (GATE_5)	55	GND	44	PFI_1		
24	GND	22	PFI_15 (SOURCE_6)	11	GND		
57	PFI_17 (UP_DOWN_5)	56	RG	45	PFI_2		
23	PFI_16 (OUT_5)						

— INPUT PMT COUNTS [BIC]
— SHIELD COUNTS
— IIC

APPENDIX E

Procedure Sample_Data_Example;

```
var cts_hnd: TaskHandle;
    cts: UInt32;
    timeouts: float64;
    f,t0,t1: int64;
    t: Real;
    Exposure_Time: extended;
begin
    Exposure_Time:=32.8;
    cts_hnd := NULL;
    timeouts := 10.0;
    cts:=0;
    DAQmxCreateTask("",addr(cts_hnd));
    DAQmxCreateCICountEdgesChan(cts_hnd,"Dev1/ctr0","",DAQmx_Val_Falling,0,DAQmx_Val_CountUp);
    DAQmxStartTask(cts_hnd);
    QueryPerformanceFrequency(f);
    QueryPerformanceCounter(t0);
    Repeat
        DAQmxReadCounterScalarU32(cts_hnd,timeouts,addr(cts),NULL);
        QueryPerformanceCounter(t1);
        t:=1000*((t1-t0)/f);
    until (t>=exposure_time);
    Count_pmt:=int(Cts);
    if (cts_hnd <> NULL) then
        begin
            DAQmxStopTask(cts_hnd);
            DAQmxClearTask(cts_hnd);
        end;
    end;
end;
```

APPENDIX F

Network of Ebert-Fastie Spectrometers on Svalbard

Instrument name	Location	HvIP2	PC
1 m Green	Longyearbyen	158.39.49.204	158.39.49.102
1 m Silver	Longyearbyen	158.39.49.203	158.39.49.107
½ m White	Longyearbyen	158.39.49.202	158.39.49.201
½ m Black	Ny-Ålesund *	-	193.156.10.172

Mask: 255.255.255.0 Gateway: 158.39.49.1 DNS: 158.39.46.248 / 158.39.47.4

* Web Camera in Ny-Ålesund

IP: 193.156.10.173 Mask: 255.255.255.192 Router: 193.156.10.129

Name: protcam.nyaal.npolar.no DNS: 158.39.46.248 / 158.39.47.4

½ m Black: protonic.nyaal.npolar.no

An upgrade of the auroral Ebert–Fastie spectrometer

F. Sigernes*, T. Svenøe*, D.A. Lorentzen[†] and L.T.W. Sigernes[‡]

*The University Courses on Svalbard, N–9170 Longyearbyen, Svalbard, Norway;

[†]Geophysical Institute, University of Alaska, Fairbanks, Alaska, USA;

[‡]University of Trondheim, Trondheim, Norway

(In preparation)

Abstract

Two auroral 1m focal length Ebert–Fastie spectrometers have been reconfigured with new controlling hardware at Poker Flat research range, Alaska (64°N, 145°W) and at Nordlysstasjonen in Adventdalen, Svalbard (78°N, 15°E), respectively. The use of high resolution stepping motors mounted to the grating shafts of the instruments combined with either a laser position tracking system or an incremental encoder are described and discussed. Both instruments were set up to measure on multiple wavelength regions of auroral emissions. It is found that the overall operational performance of the instruments as auroral spectrometers has reached a higher level. Particularly from the standpoint of flexibility in operation, mechanical stability of components, and simplicity of construction and adjustment. The ability of one spectrometer to operate on several wavelength regions with high spectral resolution, speed and sensitivity has gained new possibilities in the field of auroral spectroscopy.

Introduction

In 1889 Herman Ebert described a spectrometer using a spherical mirror and a plane grating. His sketch is reproduced in Fig. 1. and shows the instrument as a photographic spectrograph. This optical system, the Ebert monochromator, formed sharp images for a very narrow spectral range. Later in 1952 William G. Fastie improved the performance of the instrument, using curved slits instead of straight slits (Fastie, 1952). Problems of astigmatism became less, and consequently the resolution of the instrument was improved. The instrument is now known as the Ebert-Fastie spectrometer.

The 1m Ebert–Fastie spectrometer was constructed by W. G. Fastie at John Hopkins University, Maryland at the beginning of the 70's. In all five of these instruments have been produced. In 1978 one was transferred together with a $\frac{1}{2}m$ Ebert–Fastie spectrometer to Nordlysstasjonen, Svalbard from the Geophysical Institute, University of Alaska. In addition, a 1m Ebert–Fastie spectrometer was transferred to Poker Flat research range, Alaska. The $\frac{1}{2}m$ Ebert–Fastie spectrometer was constructed during the 60's deploying Fastie's findings about the improved Ebert monochromator. This spectrometer was originally constructed for rocket measurements, but numerous of these instruments have also been used for ground-based measurements.

The introduction of photon counting and computer control of these instruments was conducted by Abas G. Sivjee at Geophysical Institute, University of Alaska in the mid 70's (Sivjee et al., 1979). This work has continued during the last decade to enhance the computer control of these instruments. But the original design of the operational hardware has not changed since the instruments were installed. Data from these instruments are widely published and recognized, but in order to meet present and future requirements in auroral spectroscopy it became apparent that an upgrade was needed. Both of the 1m Ebert–Fastie spectrometers mentioned above have been further upgraded with new controlling hardware and software which depart in its major mechanical features from past equipment. This paper describes and discusses the new operational systems of the instruments. Measurements of the auroral lines N_2^+ 4278 Å 1NG (0,1), N_2^+ 4709 Å 1NG (0,2) and the Doppler shifted and broadened hydrogen line H_β 4861 Å have been carried out in order to demonstrate the performance of the instruments as auroral spectrometers at both optical sites.

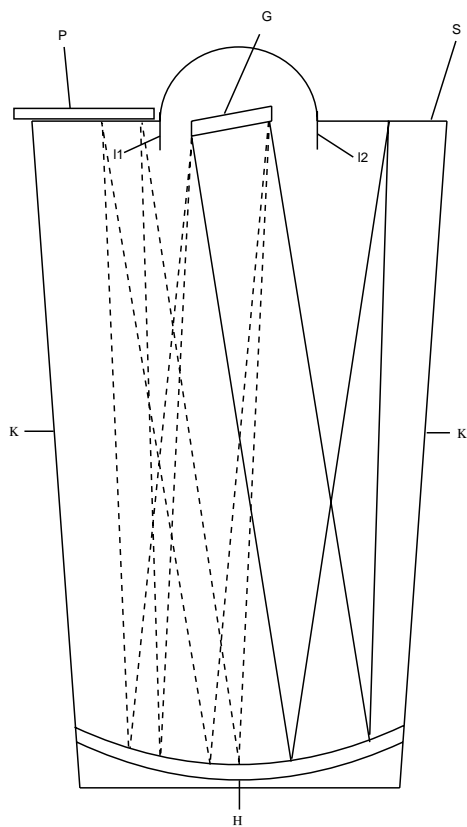


Figure 1: Reproduction of Ebert's sketch of his spectrometer. $I1$ and $I2$ are light baffles, P photographic plate, G grating, S entrance slit plane, and H spherical concave mirror. K is side plates, parts of the framework for the optical components and the housing to block stray light.

The rest of this paper contains a discussion of these results.

Optical/mechanical arrangement

The aim of the present Ebert-Fastie spectrometers is to record the emission spectra of the aurora and night-glow. Fig. 2. shows the optical arrangement of an Ebert-Fastie spectrometer. The principal components of the instrument are one large spherical mirror, one plain diffraction grating and a pair of slits. The recorded radiance from the sky, is limited by the etendue, the product of the area of the entrance slit and the field of view. Because of the low intensity of the source the

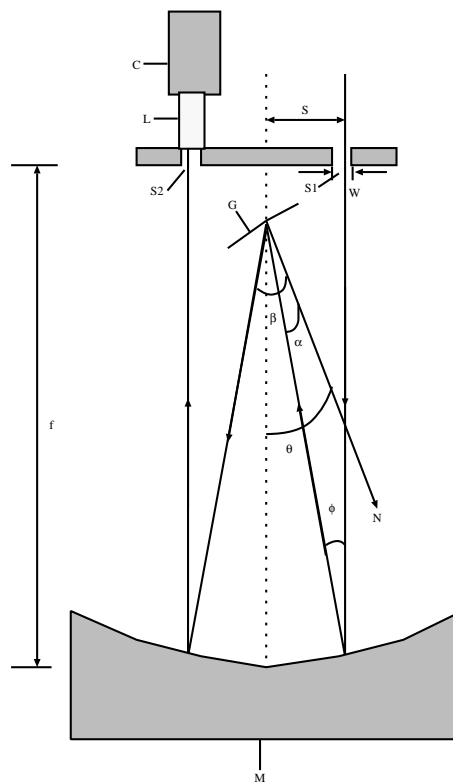


Figure 2: Arrangement of Ebert-Fastie. N is grating normal, θ grating angle, β diffraction angle, α incident angle, $2s$ distance between entrance and exit slit, w slit width, and f focal length of the spherical mirror. The focal length is ideally $\frac{R}{2}$, where R is the radius of the concave spherical mirror. ϕ is constant for given spectrometer, $\tan \phi = \frac{s}{f}$. M is spherical concave mirror, C cooled photomultiplier/housing, and L light pipe. $S1$ and $S2$ are entrance and exit slits, respectively.

etendue is made as large as possible. The image of the entrance slit is reflected and focused by one part of the spherical mirror onto the plane grating. The second part of the mirror focuses the diffracted light from the grating onto the exit slit. When the grating turns, the image of the entrance slit is scanned across the exit slit.

A light-pipe transfers the image at the exit slit to the front of a photomultiplier tube. The photomultiplier tube is mounted in a Peltier cooled housing, since sensitivity is improved by cooling the photocathode of the tube. Signals from the tube are amplified and discriminated before entering the counter card. The tubes

are of the $GaAs$ type, and the spectral response of these tubes covers a wide range from 3000 to 9300 Å. The quantum efficiency is nearly independent of wavelength. Filters in front of the entrance slit are used to prevent overlapping orders. The counter card is a daughter board designed for use with a parallel I/O baseboard for the controlling computer. The design of the counter card as a daughter board allows up to four such daughter boards to be installed on one Baseboard. The maximum count rate of this pulse counter is 32 MHz.

A picture of the upgraded Ebert-Fastie spectrometer located under a five foot dome inside the Optical Observatory at Poker Flat research range, Alaska is shown in fig. 3. This spectrometer is fixed in geographical zenith with slits aligned along the magnetic meridian. The position of the grating is controlled by a high resolution stepping motor. A full sized PC-card installed in the controlling computer gives information on acceleration, velocity and position to an Indexer. The microprocessor of the indexer uses this information to generate pulse rates up to 508,000 per second. These pulses drive the stepping motor. This technique, known as microstepping, is used to obtain high-resolution rotational motion. The motor is capable of doing 50,000 individual steps per revolution. To obtain high enough resolution on the movement of the grating a gear box, belt drive, is connected between the engine shaft and the grating shaft. This gives six times better resolution of the grating movement compared with the motor shaft. It is possible to rotate the motor/grating to a precise position and stop, rotate at a constant velocity, alternate back and forth between two angular positions or use a combination of such moves.

Additional logic provides monitoring limit switches and a home position switch. A regular Helium/Neon laser is used, combined with a mirror mounted on the motor shaft, to trigger a photoresistor to ensure the home position of the grating in zero order. An ordinary 50mm lens works as focusing element of the diverging reflected laser beam. In front of the photoresistor is a pin-hole to make sure of exact home position. This establishes an absolute reference point for the instrument, which is frequently checked during operation. A light baffle with shutter is situated in front of the entrance slit to make the field of view sufficient narrow. The upgraded 1m Ebert-Fastie spectrometer located at Nordlysstasjonen, Svalbard uses an incremental encoder instead of the laser system described above.

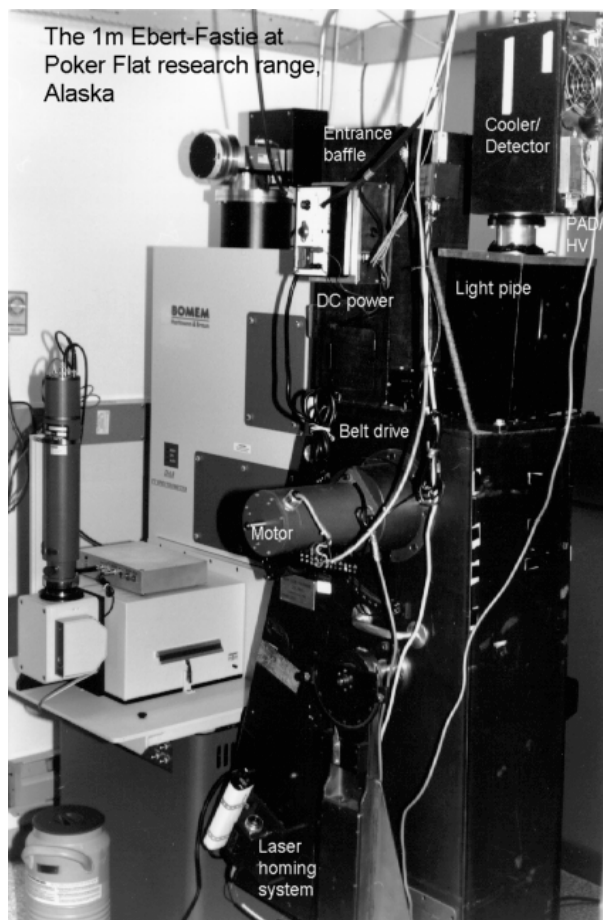


Figure 3: The upgraded blue 1m Ebert-Fastie spectrometer at Poker Flat research range, Alaska.

Fig. 4. shows the instrumental setup of this instrument together with the $\frac{1}{2}m$ Ebert-Fastie spectrometer. This motor is capable of doing 25,000 individual steps per revolution and is connected to a 5000 line encoder. The encoder shaft is mounted to a rotary table. The rotary table has a gear ratio of 1:36 and is mounted directly to the grating shaft. The same additional logic as described above provide monitoring limit switches and a home position switch by an indexer. Homing is provided by a magnetic relay mounted on the rotary table. This custom made system is capable of doing 180,000 steps per revolution of the grating with exact position tracking. The home position is therefore only checked once during an observational period.



Figure 4: The upgraded green 1m Ebert-Fastie spectrometer at Nordlysstasjonen, Svalbard. The black instrument to the right is the $\frac{1}{2}$ m Ebert-Fastie spectrometer.

The entrance optics to the spectrometers is a periscope, which can be turned in different directions along the geomagnetic meridian filling the field of view of the spectrometers. The field of view is 5 degrees.

Theory of instrument

The performance of the instrument depends on linear and angular dispersion, bandpass and calibration. The operation of a perfect instrument discussed below assumes no spherical aberration, astigmatism or grating ghosts.

The well known equation for the plane grating in

the instrument is

$$n \cdot \lambda = a (\sin \alpha + \sin \beta). \quad (1)$$

Here λ is wavelength, n spectral order, α incident angle, β diffraction angle, and a is the grating constant, see fig. 2.

Defining $\alpha = \theta - \phi$ and $\beta = \theta + \phi$ we obtain

$$\frac{d\lambda}{d\beta} = \left(\frac{a \cdot \cos \beta}{n} \right), \quad (2)$$

where $d\beta$ is the angular separation between two emissions, θ grating angle, and $d\lambda$ the wavelength separation between the two emissions. $\frac{d\lambda}{d\beta}$ is known as angular dispersion. When $d\beta$ is small, the corresponding distance in the exit plane will be $dx = f \cdot d\beta$, where f is focal length of mirror.

The linear dispersion, $\frac{d\lambda}{dx}$, is then given by

$$\frac{d\lambda}{dx} = \frac{a \cdot \cos(\theta + \phi)}{n \cdot f}. \quad (3)$$

It defines the extent to which a spectral interval is spread out across the focal plane of the spectrometer. It is associated with the ability of the instrument to resolve fine spectral detail. It is seen from equation (3) that the linear dispersion becomes smaller for higher spectral order. The bandpass BP of the instrument is defined

$$BP = \frac{d\lambda}{dx} \cdot w, \quad (4)$$

where w is the width of the exit slit. Normally the entrance and exit slits have the same width. Then BP is the instrumental line width, the half-width of a infinite narrow line passing through the instrument and recorded. By half-width is meant the full width at half maximum, FWHM. When the curved entrance and exit slits are perfectly matched, the profile of the line will be triangular.

Wavelength calibration is achieved by the use of standard emission lamps. Since the stepping motor is connected to the grating shaft through a belt or a gear drive, each step in wavelength between data points has to be calculated according to the grating equation. Between each step of the motor the grating rotates a constant angle $\Delta\theta$. If N is the total number of data points (steps) in one wavelength region and θ_1 is the start angle of the grating, then an arbitrary wavelength in this region can be found from equation (1)

$$\lambda_i = \left(\frac{2a \cdot \cos \phi}{n} \right) \cdot \sin(\theta_1 + (i - 1) \cdot \Delta\theta), \quad (5)$$

where i runs from one to N .

Using this method to obtain an intensity versus wavelength plot in one region of interest with at least two recognized/known wavelengths ξ_I and ξ_{II} , the calibrated wavelength ξ_i can be interpolated through

$$\frac{\Delta z}{\Delta z_0} = \frac{(\xi_{II} - \xi_I)}{(\xi_{II} - \xi_i)}, \quad (6)$$

where Δz is the distance between ξ_{II} and ξ_I , and Δz_0 the difference between ξ_i and ξ_{II} . Eq. (6) can only be used when there is a linear relation between wavelengths and rotation of the grating. It is now possible to find the 'true' start angle η_1 and stop angle η_N of each region. The number of data points does not change in this operation

$$\frac{\theta_N - \theta_1}{\Delta\theta} = \frac{\eta_N - \eta_1}{\Delta\eta}, \quad (7)$$

and the true step in angle, $\Delta\eta$, can be found. The calibrated values in wavelength is then simply

$$\xi_i = \left(\frac{2a \cdot \cos \phi}{n} \right) \cdot \sin(\eta_1 + (i-1) \cdot \Delta\theta \cdot \sigma), \quad (8)$$

where $\sigma = \frac{\eta_N - \eta_1}{\theta_N - \theta_1}$ can be seen has a calibration factor of $\Delta\theta$.

Ideally each photon entering the instrument will be transformed to an electronic pulse by the photomultiplier, but some loss will always occur. The throughput can be considered as an equivalent for the sensitivity or wavelength dependent calibration curve of the instrument, giving the ratio of electronic counts out to the number of photons passing through the instrument. It is necessary to calibrate the instrument against a known light source to obtain the spectral intensity in absolute units. The absolute calibration arrangement is shown in Fig. 5.

The field of view of the instrument has to be inside the fully illuminated area of the screen, which is diffusely re-emitting. $B_0(\lambda)$ is the known intensity of the Tungsten lamp in Rayleigh per Ångström, obtained at a distance r away from the lamp. The intensity $B(\lambda)$ of the screen at a distance R away from the lamp would then be

$$B(\lambda) = B_0(\lambda) \cdot \left(\frac{r}{R} \right)^2 \cdot \cos \Psi \quad \left[\frac{R}{\text{Å}} \right]. \quad (9)$$

If $C(\lambda)$ is the corresponding measured counts per unit time produced by the intensity of the Tungsten lamp, a measured auroral line with relative intensity $I_m(\lambda)$,

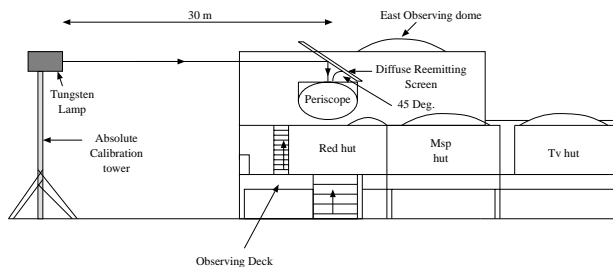


Figure 5: Absolute calibration setup. $R = 30 \text{ m}$ is distance between the calibration lamp, a Tungsten lamp, and the entrance slit normal, the vertical. $\Psi = 45^\circ$ is the angle between this vertical and the plane of the diffuse re-emitting screen.

counts per unit time, will have the intensity $I(\lambda)$ in absolute units

$$I(\lambda) = \left(\frac{B(\lambda)}{C(\lambda)} \right) \cdot I_m(\lambda) \quad \left[\frac{R}{\text{Å}} \right]. \quad (10)$$

The throughput of the instrument is influenced by the order-sorting filter at the entrance slit, because the filter itself has a characteristic transmission response dependent on wavelength. Normally compromise has to be made between ability of the instrument to resolve spectral details and expected throughput, which is also depends on the blaze angle of the grating. The most effective tilt angle of the grating is preferred. The result of the compromise is given by the resulting spectra.

Measurements and discussion

As an example of the performance of the instruments we now describe field observations of auroral spectra.

The first night of observation for the 1m Ebert-Fastie spectrometer located at Poker Flat research range, Alaska was on 17 November 1992. The optical field site at the range is operated by the University of Alaska, and is a suitable location for nighttime observations of the aurora for much of the winter season.

A diffuse auroral arc with no structure appeared in the north at about 01:00 local time (LT), and it moved fast into our field of view. The field of view of the spectrometer, looking straight up with slits aligned along the magnetic meridian, resulted in a measured area at 90 km altitude of about 9 x 12 km (Vieregk et al., 1989). The activity increased at about 02:06 LT and more structured arcs were observed. At about 03:12 LT the activity started to decrease. Fig. 6 show calibrated spectra taken during this period, comprising

(4234–4288) Å panel **A**, (4672–4740) Å panel **B**, and (4815–4884) Å panel **C**. The wavelength regions contain the auroral N_2^+ 4278 Å 1NG (0,1), N_2^+ 4709 Å 1NG (0,2), and H_β 4861 Å emission lines, respectively. Each panel is plotted as a function of time, wavelength and intensity. The intensities are given in R , and the gray-scale bars to the right indicate the intensity range of each obtained region. Also shown below each gray-scaled plot is the mean profile throughout the time period and the total intensity integrated over the whole wavelength region. The measurements are averaged in intervals of 10 minutes to increase the signal to noise ratio. All wavelength regions were obtained in the second order. The scan time for each region was about 6.0 seconds. The stepping motor used approximately 1 second to skip between different regions, which makes a total scan time of about 20 seconds. Some seconds are lost in seeking the home position after each total scan in wavelength, but is necessary in order to keep track of the exact position of the grating.

Fig. 7 shows data from the 1m Ebert-Fastie spectrometer located at Nordlysstasjonen in Adventdalen, Svalbard. During the boreal winter, the sun is more than 6 degrees below the horizon for two months, which permits optical measurements throughout the daytime and nighttime period. The instrument was set up to measure the auroral emissions H_β 4861 Å in the second order, (4800–4888) Å panel **A**, and N_2^+ 4278 Å 1NG (0,1) in the third order, (4198–4285) Å panel **B**. Also shown in fig. 7 is data from the $\frac{1}{2}$ m Ebert-Fastie spectrometer scanning in the second order, (6290–6590) Å panel **E**, throughout the whole day. The angle of the periscope was 8.2 degrees relative to the vertical pointing south, which at the site is 0 degrees relative to the geomagnetic field. The field of view is 5 degrees looking along the magnetic field lines.

On this day, the 3 of January 1995, the activity was high with great substorms on the nightside. At about 06 UT discrete morning arcs were observed followed by patchy prenoon arcs in the zenith. Again at about 08 UT the oval went south as geomagnetic noon approached. The long tail of the Doppler profile shown in panel **A** extends down to 4830 Å indicating high energy of the incoming hydrogen/proton particles. More narrow profiles about 15 Å wide appeared closer to noon, indicating that the initial proton bulk energy decreased. The rotational structure of the N_2^+ 4278 Å 1NG (0,1) emission band is clearly shown in panel **B** especially when the intensity of Hydrogen lines increases. Due to scattered sunlight the background light level rises when approaching local noon. This effect is

seen as a continuous increase in the intensity over the entire wavelength region around 12 UT in the gray-scaled plot of panel **E**.

On the 25 of January 1995 the SCIFER rocket was launched from Andøya rocket range to study ion-outflow in the prenoon region of the auroral oval. Nordlysstasjonen was used as headquarter for the campaign, and the spectrometers were operative during the launch window (See fig. 8). Again discrete morning arcs aligned north-east to south-west (geomagnetic coordinates) were observed until about 06 UT. Patchy prenoon arcs were observed to move into the field of view of the spectrometers from 06:00 to 07:30 UT. The cusp on this day was situated to the north of the station appearing at about 07:30 UT. Throughout most of the prenoon morning the spectrometers measured weak Doppler shifted auroral H_α and H_β profiles, documenting ion-inflow.

The total scan time of the 1m Ebert-Fastie at Nordlysstasjonen in Adventdalen was 60 seconds using 14 and 26 seconds in each wavelength region, respectively. The 20 seconds used between scans is necessary in order to make sure that the position tracking of the encoder is stable. After each move of the grating/motor the encoder reports the actual position according to the position counter. If an error occurs, the motor is instructed to correct its position. When the final position is reached the counters are reset and executed before the next move is conducted. It is important to initiate the indexer with the correct velocity and acceleration between different modes of movements. If the velocity or the acceleration is set to high the system becomes unstable and a stall occurs. A small backlash in the rotary table occurs when the motor/grating turns to move in the opposite direction after having obtained data from the final wavelength region. This error is less than one motor step. It is corrected by moving the motor all the way back to its home position where it again turns and moves up to its first wavelength region.

The motor of the Poker Flat instrument is rather large in physical size and strength compared to the load/grating it is moving. A large motor is more stable than a small motor due to less resonance from the indexer/motor causing instabilities in the microstepping at low speeds. There was no backlash found during operation of the instrument, which favor the use of a belt drive instead of a rotary table. The home position was checked frequently between each sweep in wavelength, and worked as an absolute reference point between scans.

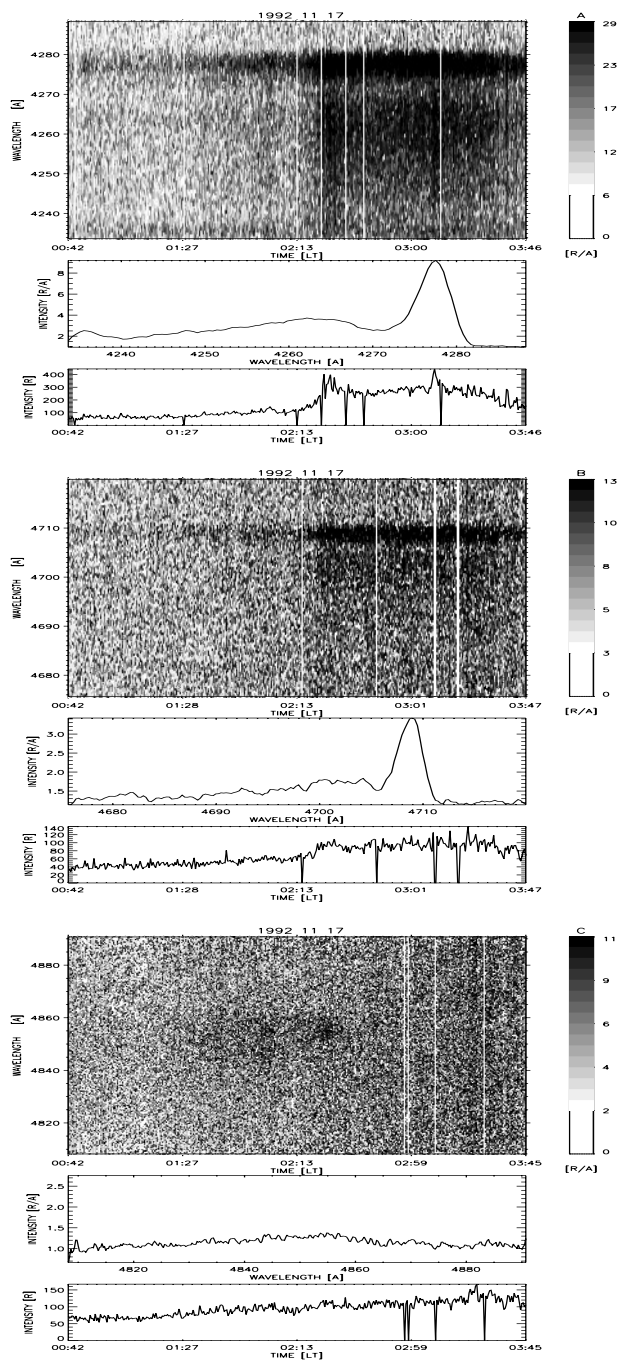


Figure 6: Spectrometer gray-scale plots for 17 November 1992 at Poker Flat research range, Alaska of the auroral emission lines N_2^+ 4278 Å 1NG (0,1) panel **A**, N_2^+ 4709 Å 1NG (0,2) panel **B**, and the Doppler shifted H_β 4861 Å panel **C** for the time period (00:42–03:45) LT. Intensities are plotted as a function of local time and wavelength. The gray-scaled bars to the right indicates the intensities in Rayleighs per Ångström. The average spectra and the total intensities are shown below each gray-scale plot.

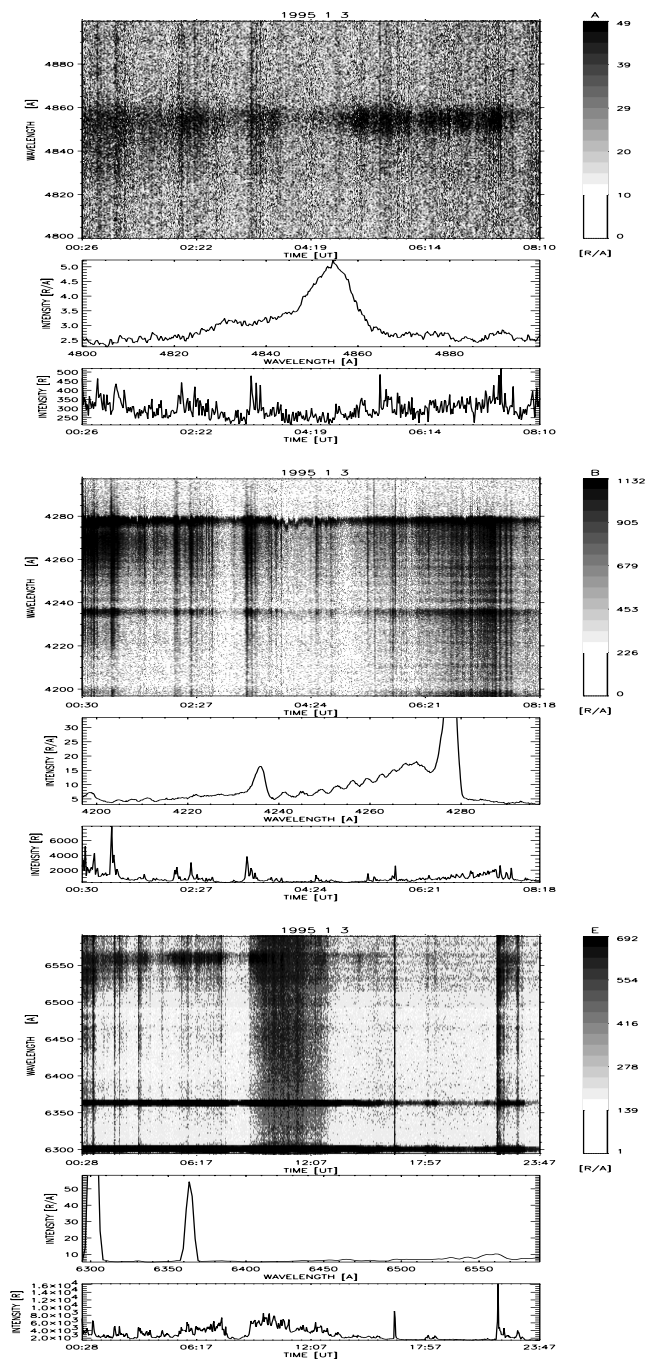


Figure 7: Spectrometer gray-scale plots for 3 January 1995 at Nordlysstasjonen in Adventdalen, Svalbard. Panel **A** shows the auroral Doppler shifted H_β 4861 Å for the time period (00:26–08:10) UT. Panel **B** shows the auroral N_2^+ 4278 Å 1NG (0,1) emission line in the time period (00:30–08:18) UT. Panel **E** shows the auroral emission lines [OI] 6300 Å, [OI] 6364 Å and the Doppler shifted H_α 6563 Å for the time period (00:28–23:47) UT. The intensities are plotted as a function of time and wavelength. The gray-scaled bars to the right indicates the intensities in Rayleighs per Ångström. The average spectra and the total intensities are shown below each gray-scale plot.

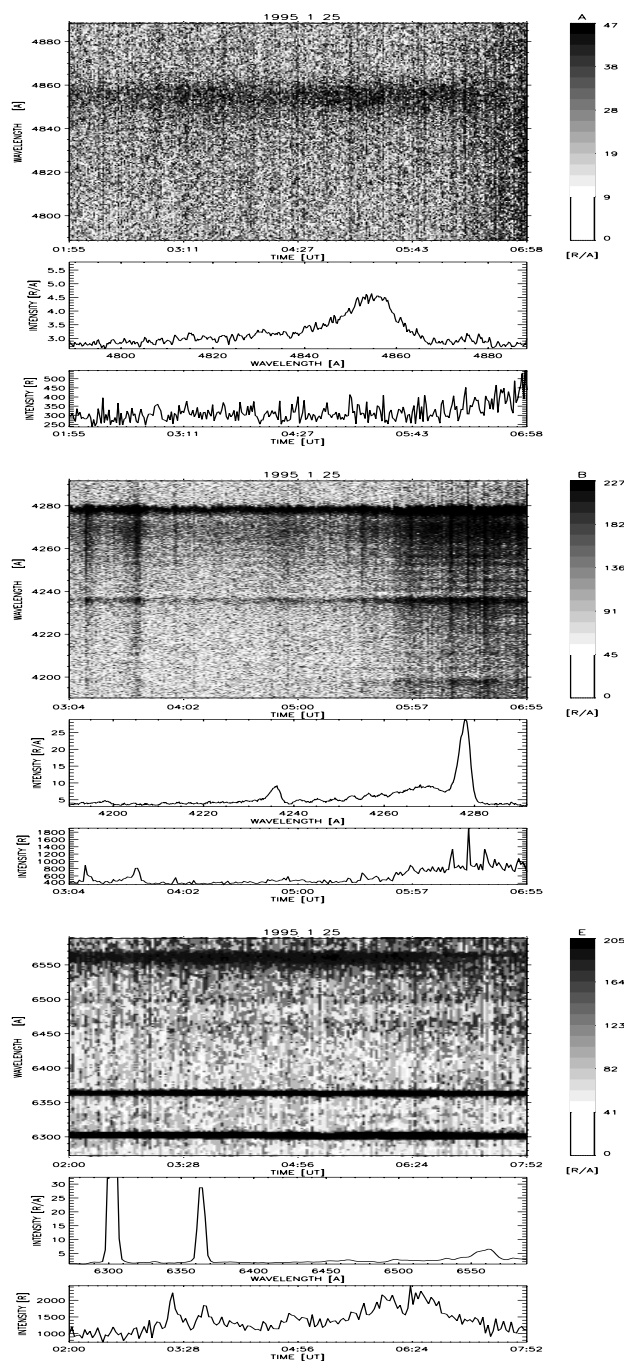


Figure 8: Spectrometer gray-scale plots for 25 January 1995 at Nordlysstasjonen in Adventdalen, Svalbard. Panel **A** shows the auroral Doppler shifted H_{β} 4861 Å in the time period (01:55–06:58) UT. Panel **B** shows the auroral N_2^+ 4278 Å 1NG (0,1) emission line for the time period (03:04–06:55) UT. Panel **E** shows the auroral emission lines [OI] 6300 Å, [OI] 6364 Å and the Doppler shifted H_{α} 6563 Å for the time period (02:00–07:52) UT. The intensities are plotted as a function of time and wavelength. The gray-scaled bars to the right indicates the intensities in Rayleighs per Ångström. The average spectra and the total intensities are shown below each gray-scale plot.

The laser homing system worked quite well, but the exact position and behavior of the motor during sampling of data was not known, producing a lack of about 1.2 Å in the bandpass of the data shown in fig. 6. This problem is eliminated by the use of a high resolution encoder.

The obtained spectra by the 1m Ebert-Fastie at Nordlysstasjonen of the auroral N_2^+ 4278 Å 1NG (0,1) emission band indicate that the bandpass is deviating about 0.5 Å to the corresponding bandpass calculated according to equation (4). It should be mentioned that a very small misalignment in the optical components of the instrument can produce the same magnitude of error in the bandpass. The motor used on the spectrometer at Nordlysstasjonen is small compared to the corresponding motor on the Poker Flat instrument, and has only twice the torque necessary to move the load. And as described earlier a small error in position may occur after each move due to resonance. If an error occurs the motor/encoder uses about 1msec to correct the position. A larger motor would not totally eliminate this problem, but a small decrease in time used between scans could be achieved. In order to do a maximum optimization a larger motor and a belt drive instead of the rotary table could be used combined with the encoder to decrease the scan time and eliminate the backlash, respectively.

Fine adjustments of the optical components in an auroral spectrometer to achieve optimal performance is often time consuming and difficult. In the near vicinity of the spectrometers hardware is setup, which enables direct access and control of the motors. It is possible to rotate the grating to a precise position and stop, look at a spectral line output image at the exit slit, adjust the optical the components, and view the result. Since the motor has a holding torque when not moving, the output spectral image at the exit slit can be improved by adjusting only one of the optical components. This makes fine tuning considerable easier than before. When the spectrometers are tuned up, adjustments of wavelength calibration is reduced to a minimum. Also, it is now possible to make the grating sequentially alternate between several narrow angular intervals. This enables one instrument to operate on more than one wavelength region.

The emissions lines N_2^+ 4278 Å 1NG (0,1), N_2^+ 4709 Å 1NG (0,2), and H_β 4861 Å were chosen to demonstrate that the upgraded spectrometers are capable of isolating any auroral emission, whether it is contaminated with overlapping emissions or weak and Doppler shifted to tens of Ångström. The ability of a spectrometer to measure several wavelength regions of auroral

emissions with high speed, resolution and sensitivity improves the possibility of obtaining corresponding exact emission ratios. Simply also, based on the fact that only one detector has to be calibrated. The intensity ratios between the Doppler shifted hydrogen lines and the N_2^+ 1NG bands, which are strongly dependent on the energy characteristics of the incoming proton flux (Rees, 1982; Van Zyl et al., 1984), can now be closely studied and used to obtain differential energy particle spectra directly from ground-based measurements.

Real-time data from the 1m Ebert-Fastie spectrometer located at Nordlysstasjonen in Adventdalen, Svalbard is available to the scientific community through *internet*.

Concluding remarks

The upgraded Ebert-Fastie spectrometers described above are improved in several aspects. The principal results obtained by this study may be summarized as follows.

1. The use of a high resolution stepping motor mounted to the grating shaft of an auroral Ebert-Fastie spectrometer combined with an incremental encoder or a laser homing system improves the overall operational performance of the instrument.
2. The ability of a stepping motor sequently to alternate a grating between narrow angular intervals makes an Ebert-Fastie spectrometer able to measure on corresponding multiple wavelength regions with high speed, resolution, and sensitivity.
3. A study of spectral emission ratios can be conducted by the use of one Ebert-Fastie spectrometer. Absolute and wavelength calibration is only necessary for one detector. Energy characteristics of incoming particle fluxes which excite the aurora can be studied in detail from ground-based observations.
4. No hands on operations is necessary in order to change setup of the instruments during an observational period, and adjustments of wavelength calibration is reduced to a minimum.
5. Fine tuning for optimal performance is no longer time consuming.
6. To achieve a minimum of instabilities in the microstepping at low speeds, the motor is recommended to have at least twice the torque necessary to move the load.
7. A belt drive is recommended instead of a rotary table between the grating shaft and the motor in order to eliminate backlash.
8. Optimal optical performance is achieved by using a high resolution encoder to enable position tracking.

Acknowledgements. Financial support for this research was provided the National Science Foundation, the Geophysical Institute, University of Alaska, NASA, The University Studies on Svalbard, and the Auroral Observatory, University of Tromsø. We would like to thank Jim Baldrige for technical assistance. The support and belief of Drs. Chuck Deehr, Roger Smith and Kjell Henriksen are appreciated.

References

- Fastie, W. G., A Small plane grating monochromator, *J. Opt. Soc. Am.*, **42**, 641, 1952.
- Fastie, W. G., Image forming properties of the Ebert monochromator, *J. Opt. Soc. Am.*, **42**, 647, 1952.
- Rees, M. H., On the interaction of auroral protons with the Earth's atmosphere, *Planet. Space. Sci.*, **30**, 463, 1982.
- Sivjee, G. G., Romick, G. J., and Rees, M. H., Intensity ratio and center wavelengths of OII (7320–7330 Å) line emissions, *Astrophys. J.*, **229**, 432, 1979.
- Van Zyl, B., Gealy, M. W., and Neumann, H., Prediction of photon yields for proton aurorae in N_2 atmosphere, *J. Geophys. Res.*, **89**, 1701, 1984.
- Viereck, R. A., and Deehr, C. S., On the Interaction between gravity waves and the OH Meinel (6–2) and the O_2 atmospheric (0–1) bands in the polar night airglow, *J. Geophys. Res.*, **94**, 5397, 1989.